



ELSEVIER

Journal of Alloys and Compounds 323 (2001) 504–508

Journal of
ALLOYS
AND COMPOUNDS

www.elsevier.com/locate/jallcom

Magnetic coupling in amorphous bilayers and sandwiches: (RCo)/Y/(RCo)' (R: Y, Gd)

L.M. Álvarez-Prado, R. Morales*, J.M. Alameda

Laboratorio de Magnetoóptica y Láminas Delgadas, Departamento de Física, Universidad de Oviedo, c/Calvo Sotelo, s/n, E-33007 Oviedo, Spain

Abstract

The magnetic behaviour of amorphous (RCo)/(RCo)' bilayers and the influence of an optional intermediate layer have been studied. In the first analysed bilayer, the monolayers have the same M_S and competing individual anisotropies, with their anisotropy axes mutually orthogonal. The magnetic coupling of YCo_2 (40 nm)/Y/ YCo_2 (40 nm)', for Y layer thickness in the 0–40 nm range, has been analyzed by bulk magnetometry and Magneto-Optic Kerr Effect. The exchange coupling produces that the easy axis of both YCo_2 layers are collinear when the intermediate Y layer is not present. On the other hand, for Y layer 2 nm in thickness, a magnetostatic coupling is observed; and, for Y intermediate layer thick enough (40 nm), no magnetic coupling is present. The second system studied is $Gd_xCo_{1-x}/Gd_{x'}Co_{1-x'}$ ($0.21 \leq x, x' \leq 0.38$). In this case the system is a Ferrimagnetic/(Ferrimagnetic)' bilayer where each individual layer has different compensation temperature. In particular for, $Gd_{0.38}Co_{0.62}/Gd_{0.21}Co_{0.79}$, the Gd magnetic subnetwork dominates at room temperature in $Gd_{0.38}Co_{0.62}$ ($T_{comp} > 300$ K), while the opposite is found for $Gd_{0.21}Co_{0.79}$ ($T_{comp} = 230$ K). The strong Co-Co exchange interaction at the bilayer interface leads to a 'macroscopic ferrimagnet behaviour'. The magnetization processes of this bilayer have also been studied. Reversible coherent rotation of the magnetization is found when the field is applied perpendicular to the easy axis of the bilayer. © 2001 Elsevier Science B.V. All rights reserved.

Keywords: Amorphous materials; Magnetic films and multilayers; Anisotropy; Magnetic measurements

1. Introduction

Magnetic coupled thin and ultrathin films, made of polycrystalline and/or amorphous layers, have received an increased interest in the last years because of its high performances as sensor devices, and its utility as model systems for testing the grounds of magnetism at different scales [1]. Here we discuss the magnetic coupling in amorphous ferro/ferro and ferri/ferri bilayers with competing anisotropies.

Samples of RCo amorphous alloys were obtained by DC magnetron sputtering on glass substrates. Each sample was prepared from pure sputtering targets, one of the targets is in front of the substrate (hereafter named 'p.d': at perpendicular deposition) and the two others making $\pm 35^\circ$ with respect to this central magnetron (hereafter named 'o.d': at oblique deposition). The base pressure of the system is $\approx 10^{-9}$ mbar, and the argon working pressure is 10^{-3} mbar.

The magnetic measurements were performed by bulk

magnetometries: vibrating sample magnetometry (VSM), and alternating gradient magnetometry (AGM); and 'surface' magnetometry: transverse magneto-optical Kerr effect (T-MOKE) on both sides of the samples. The magnetic anisotropy field, $H_K = 2 \cdot K / M_S$, was quantified from hysteresis loops and/or transverse bias initial susceptibility (TBIS) measurements [2]. Both structural (amorphicity) and morphological (sample thickness: d) characterisation of the YCo_2 layers were performed by X-ray diffraction, and the relative chemical composition was determined by electron probe microanalysis (EPMA).

2. Amorphous YCo_2/YCo_2 bilayers with competing individual anisotropies

Before the growth of the bilayers a previous study of the influence of deposition parameters on the magnetic behaviour of the related monolayers was done. Fig. 1 shows the behaviour of the anisotropy field of monolayers (in the thickness range: 10 nm–100 nm) found in amorphous thin films for the two possible positions of the Co target. These layers were grown at a deposition rate, R_v , close to 0.4

*Corresponding author. Tel.: +34-98-510-2880; fax: +34-98-510-3324.

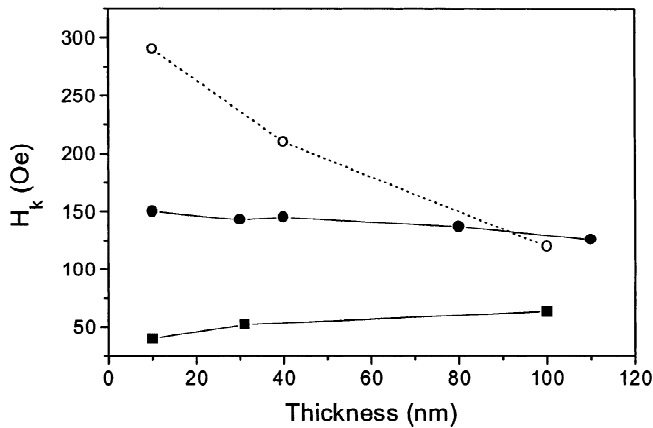


Fig. 1. Anisotropy field of the amorphous monolayers for different thickness. Open circles: Co (o.d) and Y in (p.d); Close circles: Co in (p.d) and Y in (o.d) both on glass substrates; Closed squares: Co in (o.d) on Si (100).

nm/sec. The in-plane uniaxial anisotropy, induced by growth, is transversal to the plane formed by the two incoming atomic beams. It is well known that such anisotropy is mainly caused by a self-shadowing mechanism [3]. The origin of the anisotropy will have a contribution from the film roughness; H_K is predicted to be proportional to the ratio, $\Delta^2/\lambda \cdot d$, where d is the film thickness, Δ is the averaged roughness amplitude, and λ the in-plane correlation roughness length [4,5]. Δ and λ depend on the incidence angle of the incoming atoms and the temperature of the substrate and the atomic beam [6]. As a result, the dependence of H_K with the film thickness is not, a priori, easy to predict. However from Fig. 1 it is clear that H_K increases as the angle of the effective incoming beam increases (23° for Co(o.d)–Y(p.d) and 11° for Co(p.d)–Y(o.d.) on glass substrate). Furthermore, the roughness of the substrate greatly influences the value of H_K .

In order to create bilayers with almost crossed easy axes, we turn the substrate approximately 90° after the growth of the first film. We have prepared YCo_2 bilayers from 10 nm to 100 nm thick. Here we report the magnetic properties of $\text{Y(p.d)Co}_2(\text{o.d})/\text{Y(p.d)}/\text{Y(p.d)Co}_2(\text{o.d})$, grown on glass substrates, where the thickness of the individual layers are: 40 nm for YCo_2 and 0, 2, and 40 nm for Y. The ‘p.d.’ configuration for the Y was chosen in order to avoid the self-shadowing effect in this polycrystalline layer. Table 1 shows the values of the coercive (H_c) and the anisotropy (H_K) field. When the separation layer is thick enough (i.e.: 40 nm) the YCo_2 layers behave as if they were decoupled: the two easy axes are defined by their own targets-substrate configuration and are mutually orthogonal. On the other hand, H_c and H_K are different in each layer. While the value of H_K for the first layer (grown on the glass substrate) is similar to that obtained in single layers (Fig. 1), it is greatly reduced in the second layer (grown on Y). This fact evidences the difference between metal-on-glass

Table 1
Anisotropy and coercive field for the three sandwiches reported

		H_c (Oe)	H_K (Oe)
YCo_2 (40 nm)	Second layer	90	150
Y (40 nm)	First layer	130	260
YCo_2 (40 nm)			
YCo_2 (40 nm)	Second layer	75	150
Y (2 nm)	First layer	75	240
YCo_2 (40 nm)			
YCo_2 (40 nm)	Bilayer	30	100
YCo_2 (40 nm)			

and metal-on-metal growth. The different H_c values in the sample imply that the magnetization reversal (by nucleation and domain-wall motion) is not affected by the magnetostatic coupling between both YCo_2 layers.

When the Y layer is 2 nm thick, the H_K values of the two layers are very close to that of the Y(40 nm) case, but H_c is similar in both layers. These results are qualitatively the same as those found in $\text{YCo}_2/\text{Mo}/\text{GdCo}_2$ where the thickness of the Mo layer was 2 nm [7]. It evidences the effect of the magnetostatic coupling on the magnetization reversal. Finally, direct exchange-coupled $\text{YCo}_2(40 \text{ nm})/\text{YCo}_2(40 \text{ nm})$ bilayers shows a magnetic behaviour completely different to the cited trilayers. The easy axis of the two layers are collinear and both follow the direction of the first layer’s easy axis. H_c is shared by the two layers and it is clearly lower than those in the trilayer case; this effect can be related with the total magnetic volume thickness (80 nm) of the bilayer [8]. H_K is approximately the difference of the anisotropy fields of the single layers found in the $\text{YCo}_2/\text{Y}/\text{YCo}_2$ sample (see Table 1). This result is expected for the average magnetization of a magnetic system with two mutually perpendicular uniaxial anisotropies of different magnitude [9,10].

3. Amorphous $\text{Gd}_x\text{Co}_{1-x}/\text{Gd}_{x'}\text{Co}_{1-x'}$ bilayers

We have studied magnetization processes and magnetic coupling in bilayers $\text{Gd}_x\text{Co}_{1-x}/\text{Gd}_{x'}\text{Co}_{1-x'}$ ($21 \leq x, x' \leq 38$) in the temperature range $10 \text{ K} \leq T \leq 330 \text{ K}$. The thickness for each individual layer is 100 nm. The Gd–Co anti-ferromagnetic coupling within each layer and the Co–Co ferromagnetic coupling between layers give rise to a great variety of magnetic behavior depending on temperature and composition.

Of particular interest is the behavior at room temperature (RT) of the bilayer $\text{Gd}_{0.38}\text{Co}_{0.62}/\text{Gd}_{0.21}\text{Co}_{0.79}$, which individual magnetic subnetwork at null applied field, are depicted in Fig. 2a. The preparation method (oblique incidence of incoming atom beams) induce collinear uniaxial in-plane easy axes. At room temperature, the magnetic moment of the Gd subnetwork dominates in

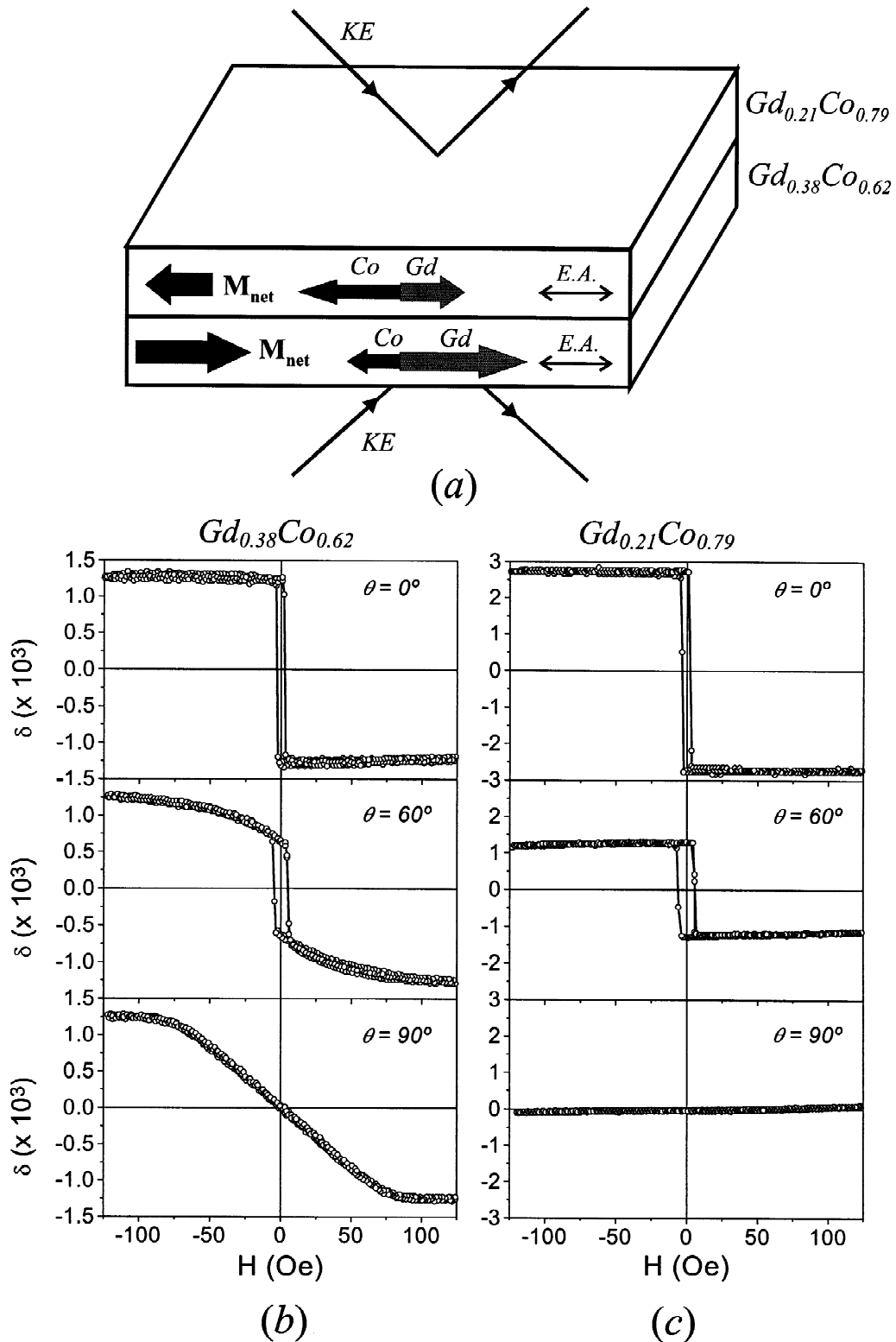


Fig. 2. (a) Magnetic configuration of the bilayer $Gd_{0.21}Co_{0.79}/Gd_{0.38}Co_{0.62}$; (b) Hysteresis loops by T-MOKE in $Gd_{0.38}Co_{0.62}$; (c) $Gd_{0.21}Co_{0.79}$.

$Gd_{0.38}Co_{0.62}$, since its compensation temperature (T_{comp}) is well above RT. However, the T_{comp} of $Gd_{0.21}Co_{0.79}$ is close to 230 K and, therefore, the Co subnetwork dominates in this alloy at RT. The Co–Co exchange interaction

at the interface aligns the Co magnetic moments of both layers, creating a magnetic system with two opposite net magnetizations (macroscopic ferrimagnet).

The magnetization processes of each individual layer

were studied by transverse magneto-optical Kerr effect (T-MOKE). The probing depth of T-MOKE is close to 40–50 nm in amorphous RE–TM alloys [11]. Hysteresis loops for fields applied at several different angles (θ) with respect to the easy axis (E.A.) are shown in Figs. 2b–c. Note that the T-MOKE parameter δ is 1.25×10^{-3} and 2.6×10^{-3} for $\text{Gd}_{0.38}\text{Co}_{0.62}$ and $\text{Gd}_{0.21}\text{Co}_{0.79}$ respectively ($\delta = \Delta R/R$ where R is the reflectivity and ΔR the magneto-optical modulation by two opposite polarities of magnetization in the transverse Kerr effect configuration).

The hysteresis loops obtained for each layer, when $\theta = 0^\circ$ and the applied fields are moderate ($H \leq 125$ Oe) (Figs. 2b,c), show that the magnetization reversal processes take place, simultaneously in both layers, by nucleation of reverse domains and 180° domain-wall sweeping. Note that, for the moderate applied fields, the hysteresis loops are both inverted. This is clearly understood if we consider two facts; first, at visible wavelengths, T-MOKE probes mainly the Co subnetwork; and, second, when a magnetic field is applied, the net magnetization of $\text{Gd}_{0.38}\text{Co}_{0.62}$ (note: $M_s(\text{Gd}_{0.38}\text{Co}_{0.62}) \approx 5 \cdot M_s(\text{Gd}_{0.21}\text{Co}_{0.79})$) follows the H direction. So, in both layers the Co magnetic moment is opposite to H , from moderate H_{max} to remanence. However, if the applied field is greater than 600 Oe the net magnetization of $\text{Gd}_{0.21}\text{Co}_{0.79}$ switches and a Bloch wall across the bilayer is present [7] (see Fig. 3a).

If a moderate magnetic field is applied at some intermediate angle between the easy and hard axes, the hysteresis loops of $\text{Gd}_{0.38}\text{Co}_{0.62}$ show the typical approach-to-saturation behavior, while those of $\text{Gd}_{0.21}\text{Co}_{0.79}$ remain square but with a reduced value of the apparent saturation magnetization (Figs. 2b,c, for $\theta = 60^\circ$). In this case, the magnetization of the $\text{Gd}_{0.38}\text{Co}_{0.62}$ layer is saturated, but the applied magnetic field is not large enough to take the magnetization of $\text{Gd}_{0.21}\text{Co}_{0.79}$ out of the easy axis significantly. For this layer, the δ value obtained at an angle θ is proportional to $\cos\theta$. Furthermore, the coercive forces (H_c) of each layer are the same for any value of θ . It

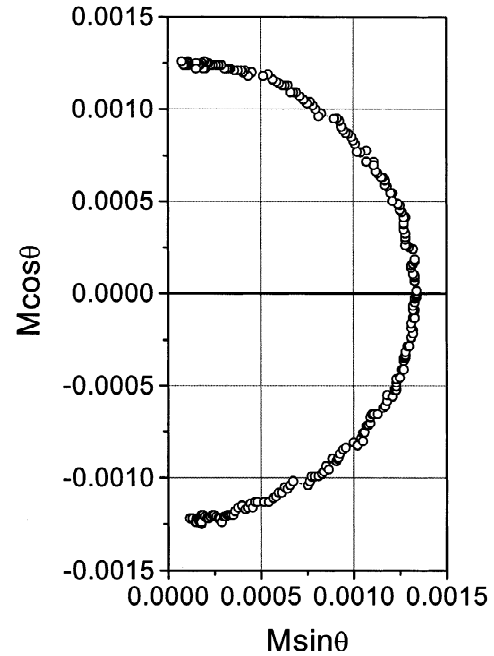


Fig. 4. Polar representation of magnetization in $\text{Gd}_{0.38}\text{Co}_{0.62}$ obtained from δ measurements along and perpendicular to the applied field.

reveals that the strong Co–Co exchange interaction produces the simultaneous switching of both layers.

When the magnetic field is applied along the hard axis ($\theta = 90^\circ$), the $\text{Gd}_{0.38}\text{Co}_{0.62}$ film is saturated at 100 Oe, while the $\text{Gd}_{0.21}\text{Co}_{0.79}$ one has a saturation field close to 3000 Oe (Figs. 2b,c, 3b). This agrees with the difference between the net magnetizations of the layers at RT and the fact that, when both magnetizations rotate towards H , a Bloch wall is formed across the bilayers thickness. This wall becomes close to 180° at $H = 3000$ Oe. The opposite slope observed in these loops is again a result of T-MOKE measurements, which are basically Co subnetwork sensitive. It is very interesting to note that the magnetization

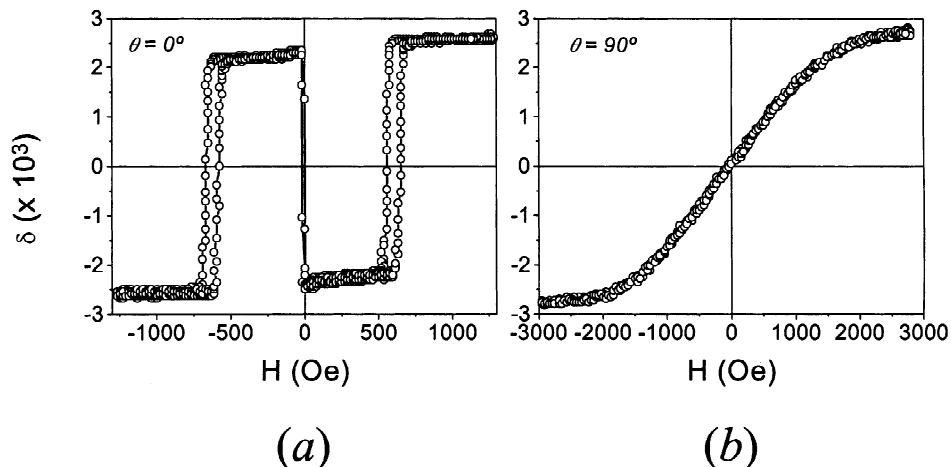


Fig. 3. Hysteresis loops by T-MOKE in $\text{Gd}_{0.21}\text{Co}_{0.79}$ along the easy (a) and hard (b) axes.

reversal process in $\text{Gd}_{0.38}\text{Co}_{0.62}$ at moderate fields occurs by reversible coherent rotation, as it is shown in Fig. 4. It presents the polar representation of magnetization obtained from the components of the magnetization along and perpendicular to the applied field.

Acknowledgements

This work is supported by the Spanish CICYT (MAT99-0724-03-02)

References

- [1] See, for example, Vol. 200 of *J. Mag. Mag. Mat.*, p. 47, p. 248, p. 322, p. 392, p. 552, p. 571, p. 583 and p. 598.
- [2] L.M. Alvarez-Prado, G.T. Pérez, R. Morales, F.H. Salas, J.M. Alameda, *Phys. Rev. B* 56 (1997) 3306.
- [3] D.O. Smith, M.S. Cohen, G.P. Weiss, *J. Appl. Phys.* 31 (1960) 1755.
- [4] E. Schömann, R.I. Joseph, *J. Appl. Phys.* 31 (1970) 1336.
- [5] Y.P. Zhao, G. Palasantzas, G.C. Wang, J.Th.M. De Hasson, *Phys. Rev. B* 60 (1999) 1216.
- [6] S. Lichter, J. Chen, *Phys. Rev. Lett.* 56 (1986) 1396.
- [7] J.M. Alameda, L.T. Baczewski, N. Bobillo, D. Givord, G.T. Pérez, F.H. Salas, *J. Mag. Mag. Mat.* 121 (1993) 336.
- [8] R.F. Sotho, *Magnetic Thin Films*, Ed. Harper and Row, 1965.
- [9] E.J. Torok, R.A. White, A.J. Hunt, H.N. Oredson, *J. Appl. Phys.* 33 (1962) 3037.
- [10] S. Rinaldi, L. Paretto, *J. Appl. Phys.* 50 (1979) 7719, For a very recent review, see also: M. Valvidares, L.M. Alvarez-Prado, J.I. Martínez and J.M. Alameda. To be published.
- [11] F.H. Salas, C. Dehesa, G.T. Pérez, J.M. Alameda, *J. Magn. Magn. Mater.* 121 (1993) 548.